Electronic Supplementary Information for:

Both protein adsorption and aggregation contribute to shear yielding and viscosity increase in protein solutions

Maria Monica Castellanos,[a] Jai A. Pathak*[b] and Ralph H. Colby*[a]

[a]Materials Science and Engineering, The Pennsylvania State University, University Park, PA, 16802, USA

[b]Formulation Sciences Department, MedImmune, 1 MedImmune Way, Gaithersburg, MD, 20878, USA

**Email: PathakJ@medimmune.com, rhc@plmsc.psu.edu*

This document contains information on the stability of the mAb used in this work, along with details regarding the fixtures of the CB rheometer, the torque balance and calculation of the *K* parameter necessary to determine interfacial contributions in bulk rheology measurements. Bulk rheology data of BSA solutions in the presence of surfactant are presented, followed by surface rheology data for solutions of BSA and mAb under different conditions: with surfactant, in the absence of surfactant (for BSA), after prolonged incubation at 40 ^{0}C (for the mAb). Finally, some comments on the limitations of the rheometers used are discussed.

Stability data of the mutated mAb

The mAb of this study correspond to an IgG1 that has three mutations in the C_H2 domain in order to enhance antibody dependent cell mediated cytotoxicity (ADCC).[1] However, the mutated mAb has lower conformational stability, and unfolding of the C_H2 domain occurs at 49 ^{o}C (see Fig. SI. 1). Differential scanning calorimetry (DSC) shows that the conformational stability of the C_H2 domain decreases from 68 to 49 ^{o}C after the mutation. Additionally, aggregation is promoted at 40 ^{o}C with more than 10 % monomers loss after 18 days at the higher concentrations.

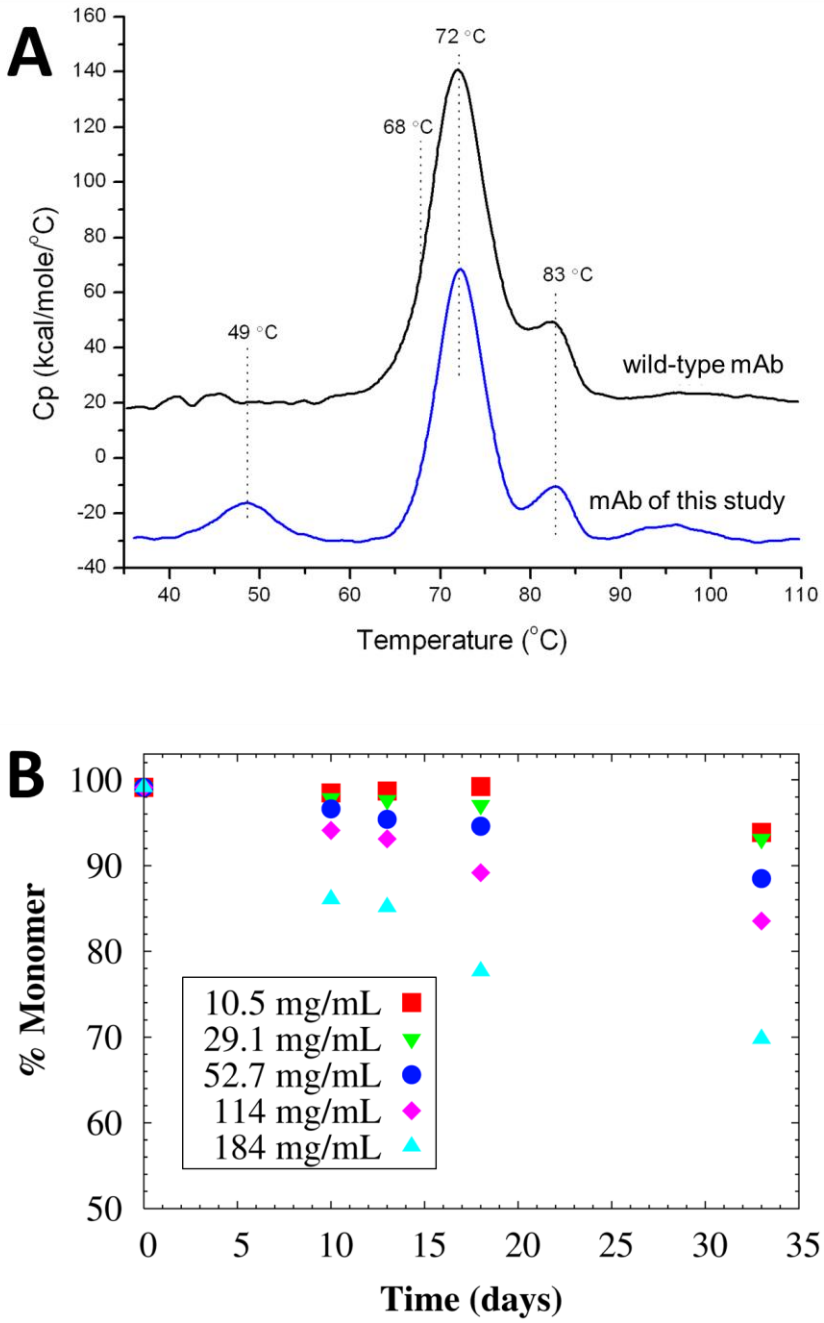

Fig. SI. 1. Stability data of the mutated mAb. **A.** Differential Scanning Calorimetry (DSC) data showing the unfolding of the mAb domains (data kindly provided by W. Leach). **B.** Percentage of monomer remaining after incubation at 40 ^{o}C, for concentrations from 10.5 to 184 mg/mL.

The mutated mAb also forms subvisible particles upon incubation at 40 ^{o}C. The micro-flow imaging (MFI) data (Fig. 7) are presented here in histogram format, showing the increase in particle concentration as the mAb is incubated at 40 ^{o}C for prolonged times.

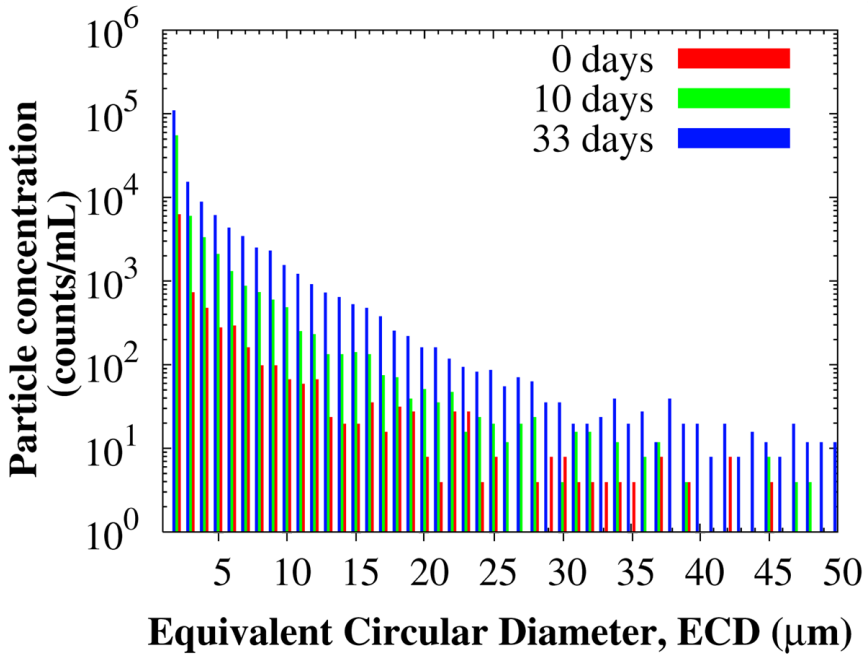

Fig. SI. 2. Concentration of subvisible particles in mAb samples at 114 mg/mL incubated at 40 ^{o}C for 0, 10 and 33 days obtained from MFI.

Effect of fixture geometry on the apparent viscosity of BSA solutions

As described in the methodology section, two fixtures of the CB rheometer (Contraves) were used in order to study bulk contributions to the apparent viscosity. Fig. SI. 3 includes a representation for each of the fixtures with lengths 8.0 mm and 15.2 mm, the latter having a higher surface area in contact with the bulk.

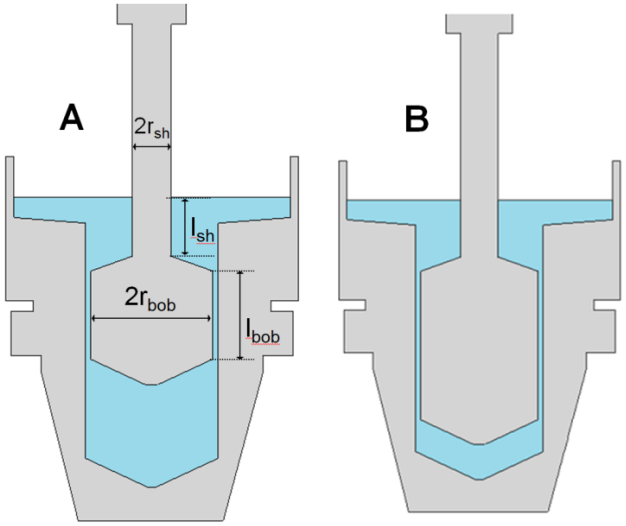

Fig. SI. 3. Schematic representation of the fixtures used in the CB rheometer. **A.** The short bob has a length of 8.0 mm, and **B.** A bob with about twice the length of the bob in A. (15.2 mm) keeping all other dimensions constant.

A torque balance provides information on the relative contributions from the bulk and the interface for a given geometry. The measured torque in the CB rheometer M_{CB} depends on the force (stress on a unit area or length, for the bulk and the interface respectively) applied at a given distance. Consider an interface with an infinitesimal thickness $\Delta \to 0$, a total stress in the CB rheometer σ_{CB}, an interfacial stress σ_S, and a bulk stress σ_B. See Fig. SI. 3 for abbreviations on the geometrical parameters. For the fixtures of the CB rheometer, the torque balance is as follows:

$$M_{CB} = M_S + M_B . \qquad \text{(SI.1)}$$

The total torque in in the CB rheometer M_{CB} corresponds to:

$$M_{CB} = \sigma_{CB}\left[\left[2\pi r_{sh}\left(l_{sh}-\Delta\right)\right]r_{sh} + \left[2\pi r_{bob} l_{bob}\right]r_{bob} + \frac{2}{3}\pi\left(r_{bob}^3 - r_{sh}^3\right) + \frac{2}{3}\pi r_{bob}^3 + \left[2\pi r_{sh}\Delta\right]r_{sh}\right], \qquad \text{(SI.2)}$$

where the first term in the parenthesis corresponds to the section of the shaft immersed in the subphase, the second term refers to the region of the bob with diameter $2r_{bob}$, the

third and fourth term correspond to the conical sections in the bob, and the fifth term refers to the region in contact with the interface. The torque at the air/water interface M_S corresponds to:

$$M_S = \sigma_S \left[2\pi r_{sh}\right] r_{sh}\,, \tag{SI.3}$$

and the torque in the bulk M_B can be expressed as:

$$M_B = \sigma_B \left[\left[2\pi r_{sh} l_{sh}\right] r_{sh} + \left[2\pi r_{bob} l_{bob}\right] r_{bob} + \frac{2}{3}\pi\left(r_{bob}^3 - r_{sh}^3\right) + \frac{2}{3}\pi r_{bob}^3 \right]. \tag{SI.4}$$

Replacing SI.2 through SI.4 in SI.1 and simplifying:

$$\sigma_{CB} = \sigma_S \frac{r_{sh}^{\,2}}{\left[l_{sh} r_{sh}^{\,2} + l_{bob} r_{bob}^{\,2} + \frac{\left(2r_{bob}^3 - r_{sh}^3\right)}{3} \right]} + \sigma_B \tag{SI.5}$$

$$\sigma_{CB} = \frac{\sigma_S}{K} + \sigma_B\,. \tag{SI.6}$$

The bulk contribution includes the torque from the shaft immersed in the subphase, the bob and its conical sections. In conical sections with small angle between the cone and the plane, the shear rate is uniform and the stress is constant. For the CB rheometer, we obtain a constant K = 11.7 cm for the short bob and K = 18.8 cm for the long bob.

Fig. SI. 4 shows the experimental results and viscosity predictions using each of the fixtures depicted in Fig. SI. 3, assuming a surfactant-free BSA solution at 44.5 mg/mL with Newtonian bulk viscosity η_∞ = 1.3 mPa s, and a viscoelastic interface that follows the Bingham model with σ_{SY} = 0.7 mPa m. These values are based on measurements using the DWR and the VROC on surfactant-free BSA solutions. For the specified system, the viscosity η can be obtained as a function of shear rate $\dot{\gamma}$:

$$\eta = \frac{\sigma_S / \dot{\gamma}}{K} + \eta_\infty\,. \tag{SI.7}$$

Higher viscosities are obtained with the short bob, which has a higher interfacial contribution than the long bob ($K_{CB,short} < K_{CB,long}$). Deviations between the model and the experimental data at the low shear rates can be attributed to the viscosity not having reached a steady condition: since protein solutions are rheopectic, the low shear rate viscosity will increase with time, until the interface reaches a steady state. Augmenting the bulk contribution in *K* by a factor of ~60% with a longer bob, still produces an apparent yield stress in the same order of magnitude. When the yield stress comes from an interfacial artifact, it can be modified by changing the geometry used, but its final effect on the apparent viscosity will also be highly dependent on the interfacial and bulk viscosities of the system.

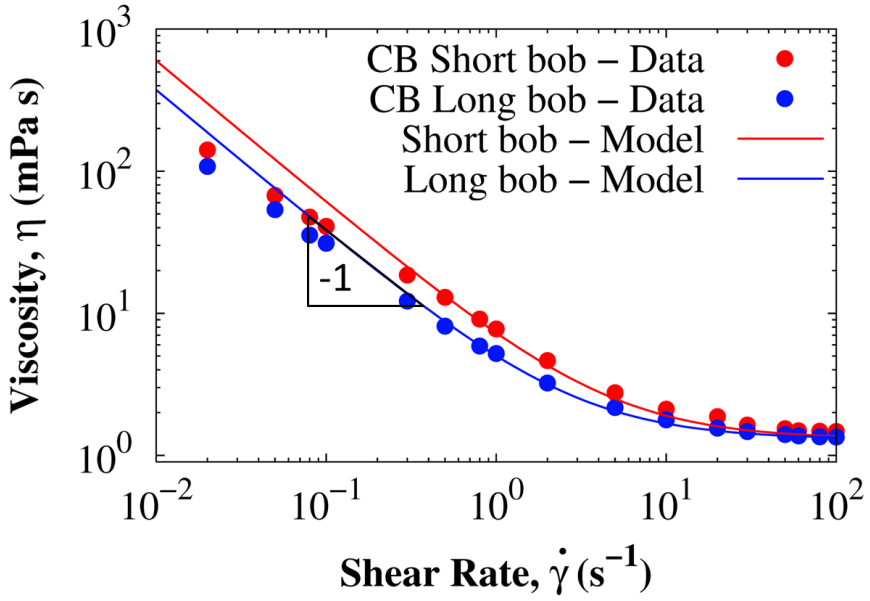

Fig. SI. 4. Apparent viscosity for a surfactant-free BSA solution using the fixtures of the CB represented in Fig. SI. 3. Points correspond to experimental data, and lines to the predictions of the model assuming a Newtonian bulk with η_∞ = 1.3 mPa s, and a viscoelastic interface that follows the Bingham model with σ_{sY} = 0.7 mPa m.

Rheology of surfactant-laden BSA

After addition of surfactant, the apparent yield stress of BSA in PBS is eliminated. Fig. SI. 5 shows that in surfactant-laden solutions, the viscosity is independent of shear rate (Newtonian response).

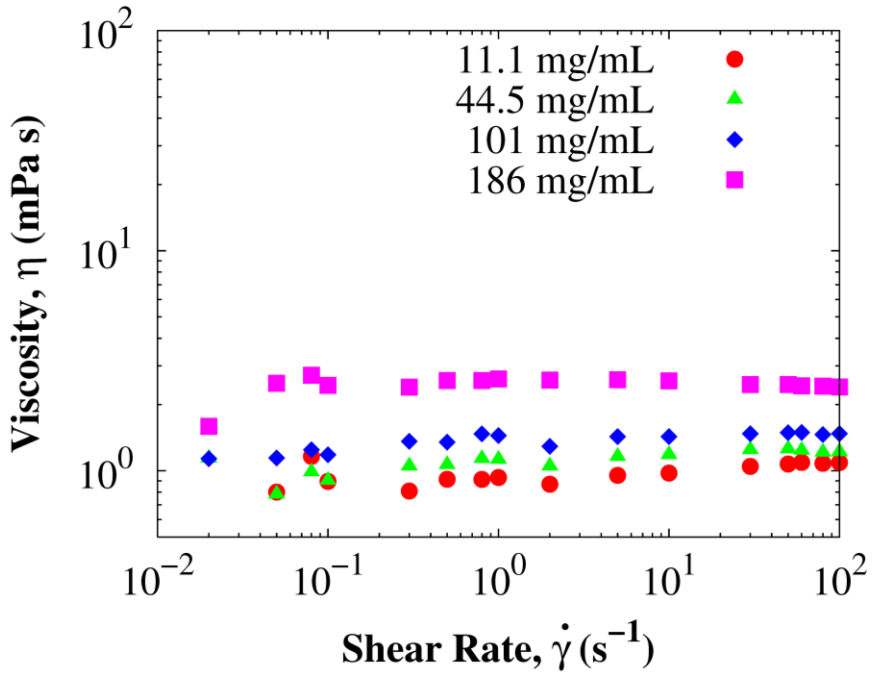

Fig. SI. 5. Rheology of surfactant-laden BSA in PBS. Addition of surfactant eliminates the apparent yield stress and the solution behaves like a Newtonian fluid.

Surface rheology of BSA solution and mAb solution

Surface rheology provides important information on the presence of viscoelastic structures at the air/water (A/W) interface that could influence the bulk measurements. Fig. SI. 6 shows the surface viscosity for the solutions of BSA and mAb studied. In the absence of the non-ionic surfactant Polysorbate 80 (PS80), a viscoelastic structure is observed. Adding surfactant decreases the surface viscosity and the yield stress by about two orders of magnitude. The small surfactant molecules are preferentially adsorbed at the A/W interface and do not display viscoelastic properties. The interfacial region is rich in surfactant PS80 and all the surfactant-laden samples have the same

surface viscosity, independent of the protein in solution. The surface viscosity of a surfactant-laden sample with 93% monomer is similar to viscosity of the sample with monomer purity of 99%. Thus, the surfactant dominates the interfacial properties even in the presence of aggregates, which is not the case for bulk rheology. The surface viscosity of surfactant-free BSA is equivalent for bulk concentrations between 11 and 186 mg/mL, as these concentrations are well above the minimum protein concentration required to reach surface coverage (data not shown).

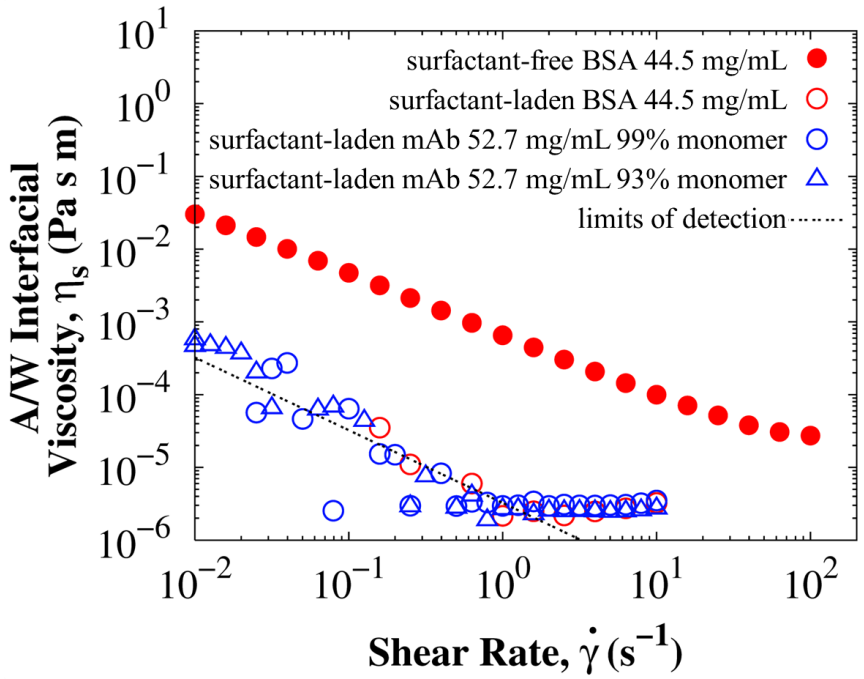

Fig. SI. 6. A/W Interfacial viscosity of BSA and mAb solutions. Surfactant-free BSA solutions are viscoelastic. However, protein-surfactant mixtures have an insignificant yield stress and the interfacial rheology is dominated by the surfactant with minimum contribution from the protein.

Limitations of rheology measurements

It was shown in the main manuscript that for the mAb sample at 114 mg/mL, the yield stress is only detected after 18 days of incubation at 40 ^{o}C. Even when a yield stress could be present in samples exposed for shorter periods of time, the MCR301 is a stress controlled rheometer that cannot measure any stress below 1 mPa. This intrinsic

limitation of the instrument does not allow the detection of a very small yield stress, and a simple calculation showed that for the sample at 52.7 mg/mL of Fig. 4A of the main manuscript, a yield stress would have been first detected only after 20 days of incubation at 40 ^{o}C.

An important consideration in the design of a rheometer fixture is minimizing surface and bulk contributions for a bulk and surface rheometer respectively. Nevertheless, the contributions of interfaces and bulk do not solely depend on the geometry, but also on the interfacial and bulk viscosities of the system. The surfactant-laden mAb solution at 52.7 mg/mL displayed similar results to those of Fig. 5B (main manuscript): the surface rheology of aggregated mAb samples was not significantly affected by the presence of aggregates. However, as the bulk viscosity increased due to protein aggregation, a higher surface yield stress was observed. Assume $\eta_S = 10^{-3}$ Pa s m for a shear rate 0.01 s^{-1} (Fig. 5B, main manuscript) and η_B of order 1 Pa s at a similar shear rate (Fig. 4, main manuscript). The resultant Boussinesq number *Bo* (see main manuscript for description) is of order 1, meaning that bulk and surface drag are equally important and the surface viscosity can be influenced by bulk effects. In fact, if one makes the reasonable assumption that the true surface viscosity of the surfactant-laden solutions is Newtonian and of order 10^{-5} Pa s m (Fig. 5B, main manuscript), *Bo* is now close to 0.01 and therefore surface measurements are substantially corrupted by the bulk. Since both bulk and surface viscosities could have surface and bulk effects respectively, the origins of the yield stress cannot be solely determined from rheology measurements, and other techniques that describe the conditions of the sample (presence of surfactants, aggregates, etc.) should be considered.

References

1. V. Oganesyan, M. M. Damschroder, W. Leach, H. Wu and W. F. Dall'Acqua, *Mol. Immunol.*, 2008, **45**, 1872-1882.